

## Degradation Mechanism of Polymer Electrolyte Fuel Cells

Minoru Inaba

Department of Molecular Science and Technology, Faculty of Engineering,  
Doshisha University, Kyotanabe, Kyoto 610-0321, Japan

\*E-mail: minaba@mail.doshisha.ac.jp

Durability is one of the most important issues in commercialization of polymer electrolyte fuel cells (PEFCs). Hydrogen peroxide formation, which is formed electrochemically or chemically during operation, is one of the potential deteriorating factors of PEFCs. It was found that hydrogen peroxide is intrinsically formed as a 2-electron reduction intermediate at Pt/C catalysts. The durability tests of the electrolyte membrane revealed that perfluorinated ion-exchange membrane is not completely stable against hydrogen peroxide, especially in the presence of  $\text{Fe}^{2+}$  and  $\text{Cu}^{2+}$  ions. Under open-circuit conditions of the single cell, the electrolyte membrane deteriorated, and it was concluded that hydrogen peroxide is formed by gas crossover and the resulting catalytic combustion, most probably at the anode side. The hydrogen peroxide decomposes chemically the electrolyte membrane, resulting in degradation of the MEA.

### 1. Introduction

Polymer electrolyte fuel cells (PEFCs) have attracted much attention for the power sources of electric vehicles and for household cogeneration systems, and are now being developed intensively for commercialization. Durability is one of the most important issues in commercialization of PEFCs. For example, a long life over 40,000 hours (= 10 years in the daily start and stop (DSS) mode) is required for PEFC stacks used in the household cogeneration systems; however, sufficient durability to meet this demand has not been established even for single cells. Various mechanisms are being considered as deteriorating factors of the cell stacks in a long-term operation. Hydrogen peroxide formation, which is formed electrochemically or chemically during operation, is one of the potential deteriorating factors of PEFCs [1]. In the fuel cell reaction, it is believed that the only product is water, which is a big advantage of PEFCs. However, it is also widely recognized that hydrogen peroxide, which is a 2-electron reduction intermediate, as well as water, which is a 4-electron reduction product, is formed in oxygen reduction reaction (ORR) as shown in Fig. 1 [2,3]. Hydrogen peroxide is a highly oxidative reagent that has a high reduction potential (1.77 V), and therefore may deteriorate materials in the membrane-electrode assembly (MEA) of PEFCs. We have focused on hydrogen peroxide as

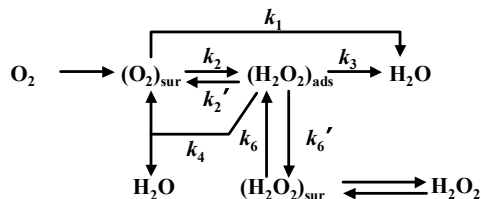


Fig. 1. Scheme for ORR [3].

a degradation factor of PEFC stacks, and have investigated durability of materials, mainly the electrolyte, used in MEAs against hydrogen peroxide and the mechanism for hydrogen peroxide formation at Pt/C catalysts. We have also studied the degradation of MEAs by operating a single cell under accelerated operating conditions. In this report, recent results on these topics are summarized.

### 2. Experimental Methods

**2.1. Durability Tests of Perfluorinated Ion-Exchange Membranes against Hydrogen Peroxide** 1 x 1 cm pieces of Nafion® 117 (DuPont, EW = 1100, thickness: 175  $\mu\text{m}$ ) membrane were used for durability tests. As swelling pretreatment, the samples were boiled successively in 3%  $\text{H}_2\text{O}_2$ , water, 1 M  $\text{H}_2\text{SO}_4$ , and water. The proton of the  $\text{H}^+$ -Nafion samples was ion-exchanged to various types of cations by immersing them in 0.1 M

chloride or nitrate solutions for more than 24 h. Each Nafion sample was immersed in 30% H<sub>2</sub>O<sub>2</sub> kept at 80°C for 12 h, and the solution were analyzed with an ion chromatograph (Dionex, DX-120).

## 2.2. Oxygen Reduction Reaction on Pt/C Catalysts

The behavior of ORR on Pt/C catalysts was analyzed by the rotating ring-disk electrode (RRDE) technique [5-7]. Commercially available catalysts of Pt (5-80 wt%) supported on Vulcan XC-72 (E-TEK) was used as catalyst samples. The nominal diameters of the Pt particles are listed in Table 1 [4]. The RRDE (Nikko Keisoku) consisted of a glassy carbon (GC) disk and a platinum ring. The collection efficiency  $N$  determined using a solution of Fe(CN)<sub>6</sub><sup>3-</sup> was  $0.36 \pm 0.02$ . The Pt/C catalyst was ultrasonically dispersed in ethanol at a concentration of 1 g dm<sup>-3</sup>. An aliquot of the suspension was carefully dropped on the GC disk electrode with a microsyringe to adjust Pt/C loadings at 5.67-56.7 μg<sub>carbon</sub>-cm<sup>-2</sup>, and dried overnight at 60°C in an electric oven.

Table 1. Nominal particle sizes and specific surface areas of Pt/C\* [4]

Pt loading / wt%	Particle size / nm	Specific surface area / m <sup>2</sup> g <sup>-1</sup>
10	2.0	140
20	2.5	112
30	3.2	88
40	3.9	72
60	8.8	32
80	25.0	11

\*No data for 5 wt% Pt/C.

A glass cell that was filled with 1.0 M HClO<sub>4</sub> was used for electrochemical measurements. The counter and reference electrodes were a Pt plate and a reversible hydrogen electrode (RHE), respectively. Electrochemical measurements were carried out using a dual-potentiostat (ALS, Model 700A) and a motor speed controller (Nikko Keisoku, RDE-1). The disk and ring potentials were scanned repeatedly between 0.0 and 1.4 V at 50 mV s<sup>-1</sup> under argon atmosphere to remove residual impurities. Current-potential relations for ORR were measured in O<sub>2</sub>-saturated solutions at various rotation rates. The potential of the GC disk was swept at 2 mV s<sup>-1</sup> in the negative-going direction from 1.0 to 0.05 V to obtain current-potential curves. The ring potential was kept at 1.4 V, at which all H<sub>2</sub>O<sub>2</sub> molecules that reached the ring

were oxidized to O<sub>2</sub>, to detect H<sub>2</sub>O<sub>2</sub> formed at the disk electrode. All measurements were carried out at 25°C.

## 2.3. Estimation of Gas Crossover and Open-Circuit Voltage Durability Tests

A single PEFC cell (25 cm<sup>2</sup>) with a MEA consisting of a perfluorinated ion-exchange membrane, Pt-Ru/C anode and Pt/C cathode was used for hydrogen crossover measurements. Humidified pure hydrogen (99.9999%) and argon (99.9999%) were fed through the anode and cathode, respectively, both at 300 mL min<sup>-1</sup>. Hydrogen crossover across the MEA was measured electrochemically. The potential of the cathode (the Ar-side) was swept at 1 mV s<sup>-1</sup> from the OCV (ca. 100 mV) to 500 mV against the anode (H<sup>+</sup>/H<sub>2</sub>). The diffusion limiting current in the range 300-350 mV was recorded as a measure of hydrogen crossover. The effects of the temperatures of the cell (40-80°C) and humidifiers (36-76°C), and the pressures of the gases (0-0.2 MPa) on hydrogen crossover were examined.

OCV durability tests were carried out using the same single cell and MEA. Humidified hydrogen and air were feed through the anode and cathode, respectively, both at 150 mL min<sup>-1</sup>. The cell was hold at 80°C, and both gases were humidified at 60°C. The cell was left at OCV for 60 days, and hydrogen crossover current was measured at every 24 h in the same manner as above. Anions eluted in the condensed water from the anode and the cathode were analyzed at every 24 h with an ion chromatography (Dionex, DX-120). The concentration of hydrogen peroxide eluted in the condensed water was also analyzed at by an enzyme method using a commercially available reagent (Kyoritsu Chemical-Check Lab., LR-H2O2-B).

## 3. Results and Discussion

### 3.1. Durability of Perfluorinated Ion-Exchange Membranes against Hydrogen Peroxide

The results of H<sub>2</sub>O<sub>2</sub> durability tests of Nafion samples with proton and transition metal ions as counterions are shown in Fig. 2. In the solutions after the tests, fluoride ion and sulfate ion were detected by ion chromatography. The former is derived from the C-F bonds, and the latter from the sulfonic acid moieties of Nafion. From the concentrations of F<sup>-</sup> and SO<sub>4</sub><sup>2-</sup>, the decomposition ratios were estimated for the C-F bonds and the sulfonic acid moieties,

assuming  $x = 8$ ,  $y = 1$ ,  $m = 1$  and  $n = 1$  of the chemical structure of Nafion shown in Fig. 3.

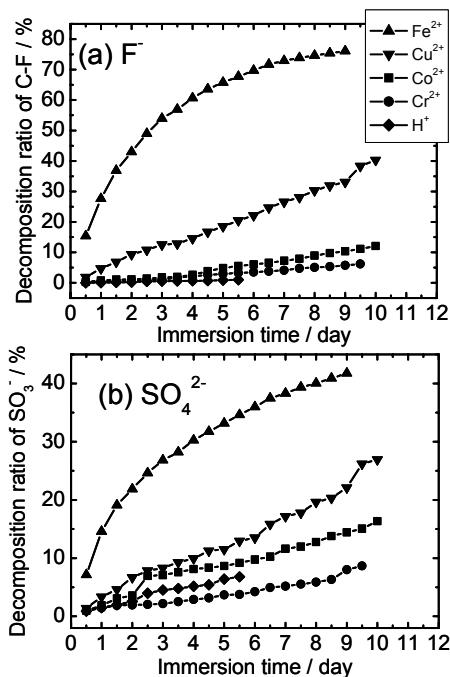


Fig. 2. Decomposition ratios of (a) C-F bonds and (b) sulfonic acid moieties of Nafion after durability test in 30%  $\text{H}_2\text{O}_2$  at  $80^\circ\text{C}$ .

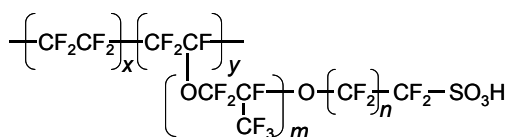


Fig. 3. Chemical structure of Nafion.

The C-F bonds for  $\text{H}^+$ -Nafion gradually decomposed with immersion time, but even after 5.5 days, the decomposition ratio was only 1%. On the other hand, the decomposition ratio of the sulfonic acid moieties was larger than that of the C-F bonds, and reached 7% after 5.5 days. It is therefore considered that the ion-exchange sites of the side-chains more easily decompose than the main chains and the ether bonds of the side chains. It should be noted that 80%  $\text{H}_2\text{O}_2$  at  $80^\circ\text{C}$  is extremely hazardous, and conventional hydrocarbon-based ion-exchange membranes would decompose explosively. The data for  $\text{H}^+$ -

Nafion in Fig. 2 proves splendid chemical stability of Nafion. Nafion samples with alkaline and alkaline-earth metal ions as counter ions showed similar results to those for  $\text{H}^+$ -Nafion (not shown in Fig. 2), which indicated that these ions have no catalytic effects for decomposition.

In the transition metal cations in Fig. 2, the results for  $\text{Co}^{2+}$  and  $\text{Cr}^{2+}$  were similar to that for  $\text{H}^+$ ; however,  $\text{Fe}^{2+}$ - and  $\text{Cu}^{2+}$ -Nafion significantly decomposed in 30%  $\text{H}_2\text{O}_2$ . In particular, more than 70% of the C-F bonds and 40% of the sulfonic acid moieties decomposed after 9 days for  $\text{Fe}^{2+}$ -Nafion. It is widely known that these ions catalytically decompose hydrogen peroxide to form hydroxyl radical [8]. For example, in the presence of  $\text{Fe}^{2+}$  ion (called the Fenton reagent)



The hydroxyl radical is strongly oxidative and works as an active species for Nafion decomposition. In Fig. 2, more than 70% of the C-F bonds decomposed, which indicates that not only the side chains, but also the main chains of Nafion were attacked by hydroxyl radical. In the case of  $\text{Cu}^{2+}$ , hydroxyl radical was formed in a similar manner.

Transition metal ions such as  $\text{Fe}^{2+}$  and  $\text{Cu}^{2+}$  are typical contaminants from piping tubes and tanks of PEFC systems. These ions accumulate in the MEA as counterions of the electrolyte membrane. Contamination with these ions should be suppressed as much as possible to achieve a long life of PEFC cell stacks.

### 3.2. Hydrogen Peroxide Formation on Pt/C Catalysts

In the MEAs, fine platinum particles (several nm in diameter) supported on carbon black (Pt/C) are used as the catalyst of the cathode and anode in PEFCs. ORR on clean bulk Pt surface has been thoroughly studied for decades [2,3,9,10], and it is widely believed that oxygen is reduced predominantly to water through direct 4-electron reduction. ORR on Pt/C catalysts has been also investigated using the rotating ring-disk electrode (RRDE) technique [11,12], and it has been reported so far that hydrogen peroxide formation is negligible (less than 1%) in the operating potential range of PEFC cathodes (0.6-0.8 V).

Figure 4 shows hydrodynamic voltammograms of RRDE with Pt/C catalysts of various Pt loadings (5-80 wt%). The loading density of Pt/C was fixed at  $56.7 \mu\text{g}_{\text{carbon}} \text{cm}^{-2}$ . The onset of the disk current

( $I_D$ ), which was consumed by oxygen reduction, was shifted to positive potentials as the Pt loading of the catalyst increased, which means an increase in catalytic activity for ORR. This is reasonable because the total amount of Pt increased with an increase in Pt loading from 5 to 80 wt%.

The ring current ( $I_R$ ), which is a measure of hydrogen peroxide formation, started to flow at around 0.8 V, and increased with a drop in disk potential. The ring current increased significantly at potential more negative than 0.2 V. In this region, the surface of Pt particle is covered with adsorbed atomic hydrogen, and it has been interpreted that the adsorbed atomic hydrogen reduces oxygen to form a large amount of hydrogen peroxide.

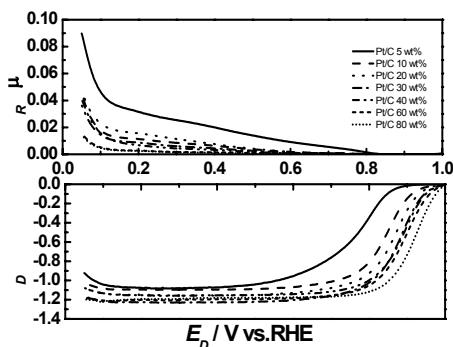


Fig. 4. Hydrodynamic voltammograms for oxygen reduction in 1 M HClO<sub>4</sub>. Disk electrodes: 5-80 wt% Pt/C (56.7 μg<sub>carbon</sub> cm<sup>2</sup>) loaded on GC, Ring electrode: Pt. Rotating rate: 900 rpm.

The ratio for H<sub>2</sub>O<sub>2</sub> formed from one oxygen molecule ( $X_{H_2O_2}$ ) at the disk electrode can be calculated using the following equation [10]:

$$X_{H_2O_2} = \frac{2I_R}{N} \bigg/ \left( I_D + \frac{I_R}{N} \right) \quad (2)$$

The variations of  $X_{H_2O_2}$  with disk potential are shown in Fig. 5. Except for 5 wt% Pt/C,  $X_{H_2O_2}$  was low (1-2%) in the normal operating potential range of PEFC cathodes (0.6-0.8 V), but increased with a drop in potential. In contrast to this, 5 wt% Pt/C produced specifically a large amount of hydrogen peroxide, and  $X_{H_2O_2}$  was about 5% in the potential range of 0.6-0.8 V.

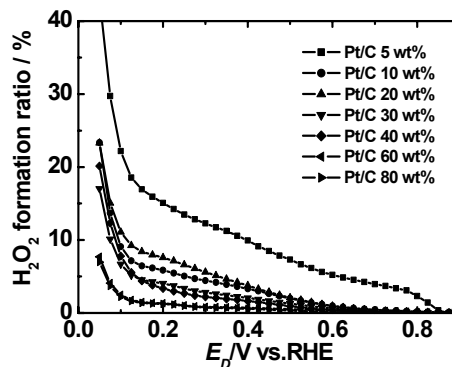


Fig. 5. The ratio of H<sub>2</sub>O<sub>2</sub> formation upon ORR at 5-80 wt% Pt/C (56.7 μg<sub>carbon</sub> cm<sup>2</sup>) loaded on GC in 1 M HClO<sub>4</sub>.

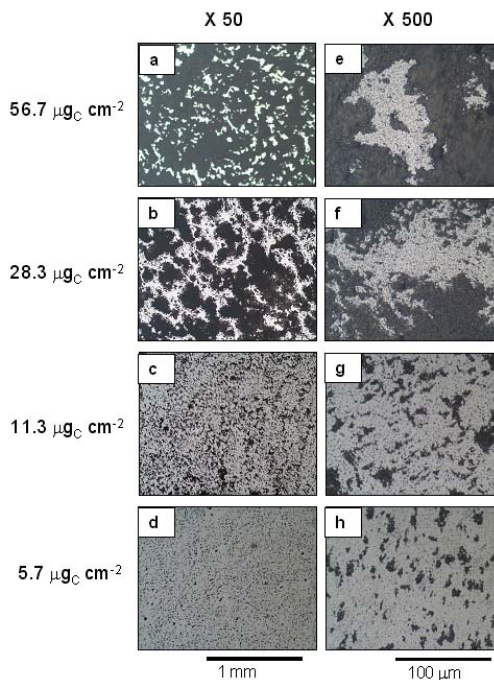


Fig. 6. Optical micrographs of 20 wt% Pt/C dispersed on GC. Pt/C loadings: (a, e) 56.7, (b, f) 28.3, (c, g) 11.3, and (d, h) 5.7 μg cm<sup>-2</sup>.

To understand hydrogen peroxide formation on Pt/C in more detail, the effect of dispersion of Pt/C catalysts on GC were examined [7]. Figure 6 shows optical micrographs of 20 wt% Pt/C catalysts dispersed on GC with different amounts. The

catalysts loaded with  $56.7 \mu\text{g}_{\text{carbon}} \text{cm}^{-2}$  were highly agglomerated, and formed a thick layer on GC (Figs. 6a and e). The agglomeration decreased with a decrease in the loading amount of Pt/C, and bare part of GC surface increased. The catalysts loaded with  $5.7 \mu\text{g}_{\text{carbon}} \text{cm}^{-2}$  seemed highly dispersed at a low magnification ( $\times 10$ , Fig. 6d); however, agglomerates of about  $10 \mu\text{m}$  were still observed at a high magnification ( $\times 500$ , Fig. 6f).

The variations of  $X_{\text{H}_2\text{O}_2}$  with disk potential are shown in Fig. 7.  $X_{\text{H}_2\text{O}_2}$  increased with decreasing the loading amount of Pt/C catalysts, and even in the normal operating potential range of PEFC cathodes (0.6-0.8 V), GC disks with the lowest Pt/C loading ( $5.7 \mu\text{g}_{\text{carbon}} \text{cm}^{-2}$ ) produced hydrogen peroxide as high as 10%. On the other hand,  $X_{\text{H}_2\text{O}_2}$  with the highest Pt/C loading ( $56.7 \mu\text{g}_{\text{carbon}} \text{cm}^{-2}$ ) produced a negligibly small amount (1%) of hydrogen peroxide. The ratio  $X_{\text{H}_2\text{O}_2}$  increased with lowering potential, and increased significantly in the  $\text{H}_{\text{upd}}$  region. Surprisingly, 65% of oxygen molecules were transformed to  $\text{H}_2\text{O}_2$  at  $5.7 \mu\text{g}_{\text{carbon}} \text{cm}^{-2}$  Pt/C loaded on GC.

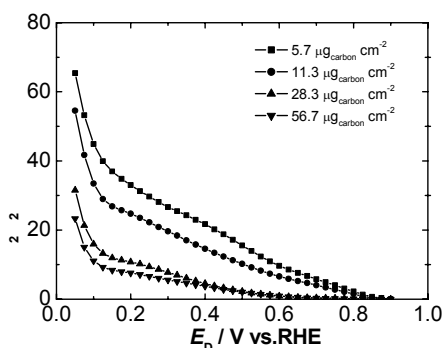


Fig. 7. The ratio of  $\text{H}_2\text{O}_2$  formation upon oxygen reduction at 20 wt% Pt/C ( $56.7$ ,  $28.3$ ,  $11.3$ , and  $5.7 \mu\text{g} \text{cm}^{-2}$ ) loaded on GC in  $1 \text{ M HClO}_4$ .

Cathodic  $\text{O}_2$  reduction is a multi-electron reaction associated with the formation of many intermediates as shown in Fig. 1 [2,3]. It has been believed for decades that oxygen is reduced to water predominantly via direct 4-electron reduction at clean bulk Pt surface except in the  $\text{H}_{\text{upd}}$  region [2,3,9,10]. Nevertheless, the results obtained in the present study revealed that 2-electron reduction pathway leading to  $\text{H}_2\text{O}_2$  formation does exist on Pt

particles supported on carbon. On hydrogen peroxide formation,  $(\text{H}_2\text{O}_2)_{\text{ads}}$  is desorbed from Pt surface, and diffuses away to the bulk of the solution. When Pt/C catalysts are highly agglomerated, the diffusing  $\text{H}_2\text{O}_2$  molecules easily meet nearby Pt/C particles, where they are transformed to water by further 2-electron reduction (series 4-electron reduction) or catalytic decomposition. Both processes lead to apparent 4-electron reduction. As mentioned earlier, in most of the studies on ORR on Pt/C catalysts, it has been reported that hydrogen peroxide formation in the normal operating potential range of PEFC cathodes (0.6-0.8 V) is negligible (less than 1%) [11,12]. In these studies, a large amount of Pt/C was loaded on GC and hence Pt/C catalysts should have been highly agglomerated. It should be noted that about 10% of oxygen was transformed to  $\text{H}_2\text{O}_2$  on  $5.7 \mu\text{g}_{\text{carbon}} \text{cm}^{-2}$  Pt/C at 0.6 V in the present study. As shown in Fig. 1, even  $5.7 \mu\text{g}_{\text{carbon}} \text{cm}^{-2}$  Pt/C was not free from agglomeration, and it is therefore reasonable to think that more  $\text{H}_2\text{O}_2$  would be produced on a single Pt/C particle. The mechanism for the appearance of the 2-electron reduction pathway on Pt/C is not clear at present, but it may originate from (i) particle size effects of platinum or (ii) interactions between Pt particles and the substrate (carbon). Further investigation on the mechanism for  $\text{H}_2\text{O}_2$  formation is needed to minimize  $\text{H}_2\text{O}_2$  formation on Pt/C and to improve the durability of MEAs of PEFCs.

**3.3. Gas Crossover and Its Effects on Degradation of MEAs** The effects of cell temperature and humidification on hydrogen crossover across the MEA at atmospheric pressure are shown in Fig. 8. Hydrogen crossover current increased with increasing cell temperature and humidification. At cell temperatures at  $70^\circ\text{C}$  or lower, humidification greatly affected hydrogen crossover current; however, it did not so much at  $80^\circ\text{C}$ . A typical amount of crossover hydrogen was about  $0.8 \text{ mA cm}^{-2}$  at a cell temperature of  $80^\circ\text{C}$  at atmospheric pressure. The increase in crossover current is probably due to softening of the membrane with an increase in temperature and swelling of the membrane with an increase in humidification. The minor dependence on humidification at  $80^\circ\text{C}$  suggests that the membrane is rather soft even at low humidification.

Figure 9 shows the effect of gas pressure on hydrogen crossover when the pressures of both gases are equal to each other. Hydrogen crossover

current increased drastically with an increase in gas pressure. At 0.20 MPa, the crossover current was 5 times higher ( $4.7 \text{ mA cm}^{-2}$ ) than that at ambient pressure. Even when slightly pressurized (e.g., at 0.05 MPa), the crossover current doubled.

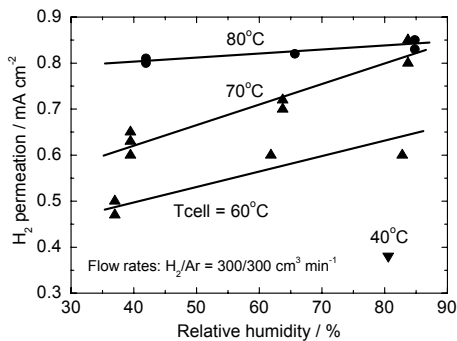


Fig. 8. Effect of cell temperature and humidification on  $\text{H}_2$  crossover current. Atmospheric pressure,  $\text{H}_2/\text{Ar} = 300/300 \text{ mL min}^{-1}$ .

Gas crossover most significantly occurs under open-circuit conditions without electrochemical reactions. We therefore carried out OCV durability tests as an accelerated operating condition. The variation of OCV during an OCV durability test is shown in Fig. 10. The cell temperature was  $80^\circ\text{C}$ , and both hydrogen and air were humidified at  $60^\circ\text{C}$  in this test. The initial OCV was about 960 mV, but it decreased gradually with an elapse of time, and dropped down to 860 mV at 1400 h. The average voltage degradation ratio of OCV was  $71 \text{ mV}/1000 \text{ h}$ , which clearly indicates that the MEA deteriorates under OCV conditions and gas crossover is one of the important degradation factors.

The variation of hydrogen crossover current during the OCV durability test is shown in Fig. 11. The crossover current was low ( $0.8 \text{ mA cm}^{-2}$ ) for initial 30 days. However, it increased rapidly after 30 days, and reached  $10 \text{ mA cm}^{-2}$  after 60 days. The increase in hydrogen crossover indicates that the electrolyte membrane deteriorated under open-circuit conditions. In the condensed water from the anode and cathode, fluoride ion was detected. Figure 12 shows the variations of the production rate of fluoride ion per day ( $\text{mg day}^{-1}$ ), which was calculated from the concentration of  $\text{F}^-$  and the volume of the condensed water. The production rate was initially  $0.05 \text{ mg day}^{-1}$ , and increased to

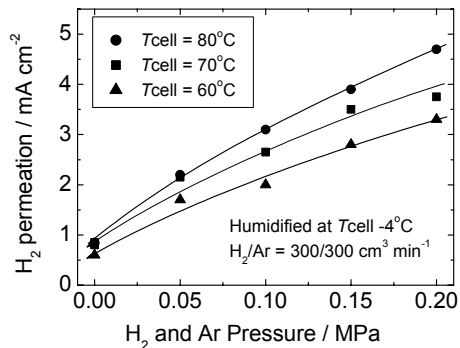


Fig. 9. Effect of gas pressure on  $\text{H}_2$  crossover current.  $P_{\text{H}_2} = P_{\text{Ar}}$ ,  $\text{H}_2/\text{Ar} = 300/300 \text{ mL min}^{-1}$ .

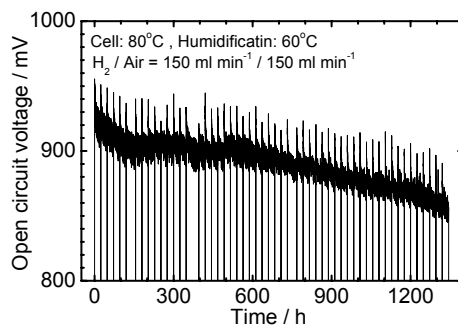


Fig. 10. Variation of OCV during OCV durability test. MEA:  $25 \text{ cm}^2$ , Cell temp:  $80^\circ\text{C}$ , humidification:  $60^\circ\text{C}$ , Atmospheric pressure,  $\text{H}_2/\text{Air} = 150/150 \text{ mL min}^{-1}$ .

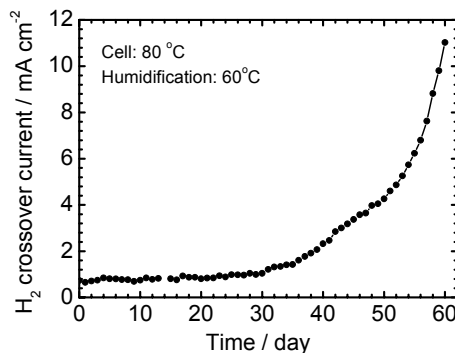


Fig. 11. Variation of  $\text{H}_2$  crossover current during OCV durability test. MEA:  $25 \text{ cm}^2$ , Cell temp:  $80^\circ\text{C}$ , humidification:  $60^\circ\text{C}$ , Atmospheric pressure,  $\text{H}_2/\text{Air} = 150/150 \text{ mL min}^{-1}$ .

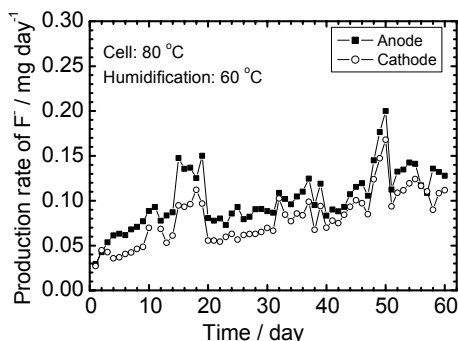


Fig. 12. Production rates of fluoride ion in condensed water from the anode and cathode during OCV durability test. MEA: 25 cm<sup>2</sup>, Cell temp: 80°C, humidification: 60°C, Atmospheric pressure, H<sub>2</sub>/Air = 150/150 mL min<sup>-1</sup>.

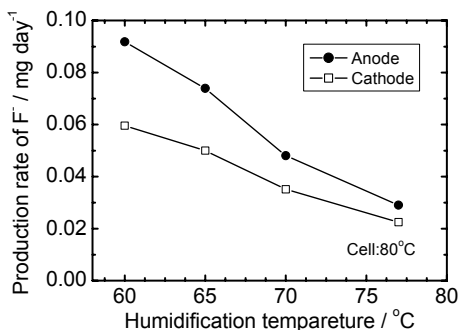


Fig. 13. Effect of humidification temperature on the production rates of fluoride ion during OCV durability test. MEA: 25 cm<sup>2</sup>, Cell temp: 80°C, Atmospheric pressure, H<sub>2</sub>/Air = 150/150 mL min<sup>-1</sup>.

0.1 mg day<sup>-1</sup> after 50 days. The fluoride ion was derived from the perfluorinated ion-exchange membrane, and hence its presence in the condensed water indicates that the membrane decomposed not physically, but chemically. It should be noted that the production rate of F<sup>-</sup> from the anode was always higher than that from the cathode. Sulfate ion was not detected in the condensed water from both the anode and cathode, which suggests that fluoride ion is released in the form of volatile HF molecules.

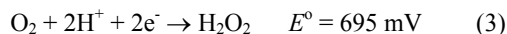
The effects of humidification temperature on the production rate of F<sup>-</sup> upon OCV tests are shown in Fig. 13. The temperature of the cell was fixed at 80°C. Both hydrogen and air were humidified at equal temperatures. As is clearly shown in Fig. 13,

F<sup>-</sup> production rate increased with a decrease in humidification, which indicates that the membrane deteriorated more significantly at lower humidification. The F<sup>-</sup> production rate from the anode was higher than that from the cathode, which was in agreement with the results in Fig. 11. In addition, hydrogen peroxide was detected (0.04 ppm) in the condensed water from the anode at a humidification temperature of 60°C.

These results of the OCV durability tests indicate that crossover of hydrogen and oxygen, and their direct catalytic combustion are the main cause of decomposition of the electrolyte membrane. Two mechanisms are possible to consider. One is thermal degradation caused by heat generation on the direct combustion, and the other is chemical degradation caused by hydrogen peroxide that is formed upon the direct combustion.

Hydrogen crossover current was of the order of 1 mA cm<sup>-2</sup> as shown in Fig. 8 at 80°C. The heat generation on the direct combustion can be calculated as: 1.481 V × 1 mA cm<sup>-2</sup> = 1.48 mW cm<sup>-2</sup>. This value is negligibly lower than heat generation under normal operation conditions. For example, when a single cell produces 300 mA cm<sup>-2</sup> at 0.74 V, heat generation is: (1.481 - 0.74) V × 300 mA cm<sup>-2</sup> = 222 mW cm<sup>-2</sup>. Hence heat generation upon the direct combustion is not a main reason for the degradation of the membrane, at least in the early stage of OCV tests. When degradation proceeds further and micro-holes are formed in the membrane, gas crossover becomes much more vigorous, and heat generation upon the direct combustion will cause a fatal damage to the MEA.

On the other hand, hydrogen peroxide was detected during OCV tests as mentioned above, and hydrogen peroxide is a potential deteriorating factor. There is a possibility that hydrogen peroxide is formed both at the cathode and the anode upon the direct combustion, as was shown in Section 3.2. The standard electrode potential of hydrogen peroxide formation is:



The potential of the cathode catalysts under open-circuit conditions was initially higher than 900 mV, and therefore hydrogen peroxide must not be formed at the cathode. On the other hand, hydrogen peroxide formation at Pt/C catalysts greatly increased at potentials more negative than 0.2 V, as shown in Section 3.2. The potential of the anode catalysts under open-circuit conditions is

nearly 0 V, and the catalyst surface is covered with atomic hydrogen. In addition, as was shown in Figs. 12 and 13, the production rate of fluoride ion was always larger from the anode than from the cathode. On the basis of these facts, it is reasonable to consider that hydrogen peroxide at the anode catalysts would have been mainly formed at the anode catalysts.

#### 4. Conclusions

We found that hydrogen peroxide is intrinsically formed as a 2-electron reduction intermediate at Pt/C catalysts. The durability tests of the electrolyte membrane revealed that perfluorinated ion-exchange membrane is not completely stable against hydrogen peroxide, especially in the presence of  $\text{Fe}^{2+}$  and  $\text{Cu}^{2+}$  ions. Decomposition of the electrolyte membrane produce fluoride ion, probably in the form of HF, which in turn may deteriorate other materials used in MEAs and cell stacks. Hydrogen peroxide formation should be minimized to attain a long life of PEFC stacks, and it is therefore very important to understand the mechanism for hydrogen peroxide formation at Pt/C catalyst in more detail. It is also beneficial to prevent contamination of  $\text{Fe}^{2+}$  and  $\text{Cu}^{2+}$  ions.

Under open-circuit conditions of the single cell, the electrolyte membrane deteriorated though no apparent electrochemical reactions occur at the cathode and anode. Hence gas crossover is one of the key deteriorating factors. We concluded that hydrogen peroxide is formed by gas crossover and the resulting catalytic combustion, most probably at the anode side. Hydrogen peroxide decomposes chemically the electrolyte membrane, resulting in degradation of the MEA. However, there still remained many questions to be answered. For example, why does the electrolyte membrane deteriorate more under dry conditions? Or what works as a catalyst for hydrogen peroxide decomposition to form hydroxyl radicals? These points should be clarified as soon as possible.

Finally, hydrogen peroxide formation was investigated as a deteriorating factor of PEFC stacks in the present study. However, there are many other deteriorating factors, depending on the operating conditions of PEFCs. Other deteriorating factors and their deterioration mechanisms should be also clarified to attain a long life of PEFCs for commercialization in the near future.

#### Acknowledgements

This work was supported by Research and Development of Polymer Electrolyte Fuel Cells from New Energy and Industrial Technology Development Organization (NEDO), Japan.

#### References and Notes

- [1] A. B. LaConti, M. Mamdan, and R. C. McDonald, in *Handbook of Fuel Cells, Vol. 3*, W. Vielstich, H. A. Gasteiger, A. Lamm, Eds. (John Wiley & Sons, New York, 2003) pp.648-662.
- [2] A. Damjanovic, in *Modern Aspects of Electrochemistry, Vol. 5* (Plenum Press, New York, 1969) pp.369-483.
- [3] M. R. Tarasevich, A. Sadkowsky, and E. Yeager, in *Comprehensive Treatise of Electrochemistry, Vol. 7* (Plenum Press, New York, 1983) pp.301-398.
- [4] E-TEK, Company catalogue (2003).
- [5] J. Maruyama, M. Inaba, and Z. Ogumi, *J. Electroanal. Chem.*, **458**, 175 (1998).
- [6] J. Maruyama, M. Inaba, T. Morita, and Z. Ogumi, *J. Electroanal. Chem.*, **504**, 208 (2001).
- [7] M. Inaba, H. Yamada, J. Tokunaga, and A. Tasaka, *Electrochem. and Solid-State Lett.*, **7**, A474 (2004).
- [8] W. C. Schumb, C. N. Satterfield and R. L. Wentworth, in *Hydrogen Peroxide* (American Chemical Society Monograph Series, 1955) p. 492.
- [9] N. M. Markovic and P. N. Ross, *Surface Science Reports*, **45**, 117 (2002).
- [10] N. M. Markovic, H. A. Gasteiger, and P. N. Ross, *J. Phys. Chem.*, **99**, 3411 (1995).
- [11] U. A. Paulus, T. J. Schmidt, and H. A. Gasteiger, and R. J. Behm, *J. Electroanal. Chem.*, **495**, 134 (2001).
- [12] O. Antoine and R. Durand, *J. Appl. Electrochem.*, **30**, 839 (2000).